Sharing the π-Bonding. An Iron Porphyrin Derivative with Trans, π-Accepting Axial Ligands. Synthesis, EPR and Mössbauer Spectra, and Molecular Structure of Two Forms of the Complex Nitronitrosyl(α,α,α,α-tetrakis(*o*-pivalamidophenyl)-porphinato)ferrate(II)

Habib Nasri,[†,‡] Mary K. Ellison,[†] Shuxian Chen,[§] Boi Hanh Huynh,*[,§] and W. Robert Scheidt*[,†]

Contribution from the Department of Chemistry and Biochemistry, University of Notre Dame, Notre Dame, Indiana 46556, and Department of Physics, Emory University, Atlanta, Georgia 30322

Received November 7, 1996. Revised Manuscript Received March 15, 1997[⊗]

Abstract: The reaction of the iron(II) picket fence porphyrin derivative $[Fe(TpivPP)(NO_2)]^-$ (Nasri et al. *J. Am. Chem. Soc.* **1991**, *113*, 717) with NO has been examined. The result is a new hexacoordinated iron(II) porphyrin complex, $[Fe(TpivPP)(NO_2)(NO)]^-$. This compound has been characterized by UV−vis, IR, EPR, and Mössbauer spectroscopies. All data show that the species is low spin ($S = {}^1/_2$). The EPR spectrum of $[Fe(TpivPP)(NO_2)(NO)]^-$ (frozen chlorobenzene solution) is similar to that of five-coordinate nitrosyl derivatives of iron(II) porphyrinates with $g_x = 2.085$, $g_y = 2.032$, $g_z = 2.01$, a_x (^{14}N) = 24 G, $a_y = 16.5$ G, and $a_z = 16$ G. Two crystalline forms of $[Fe(TpivPP)(NO_2)(NO)]^-$ were obtained and their molecular structures determined. In both crystalline forms, the axial nitro ligand is inside the "pocket" of the picket fence porphyrin derivative. In the first crystalline form isolated, there are two independent molecules, one of which has disorder in the nitro and nitrosyl groups while the other molecule has completely ordered axial ligands. In this first form, the plane of the nitro group is nearly perpendicular to the plane containing the nitrosyl group and the iron. In the second crystalline form, however, the two axial ligand planes are nearly parallel. Mössbauer investigations (solid state) show that the iron centers in the two different crystalline forms have different electronic properties. The Mössbauer parameters for the perpendicular form are $\delta = 0.22$ mm/s and $\Delta E_q = 1.78$ mm/s (200 K) and for the parallel form $\delta = 0.35$ mm/s and $\Delta E_q = 1.2$ mm/s (4.2 K). Mössbauer data are also presented for a related complex: five-coordinate [Fe(TPP)(NO)] (TPP = *meso*-tetraphenylporphinato). IR spectra for the two forms also reveal distinctly different interactions of the trans (nitro) ligand.

Introduction

There has been a surge of renewed interest in the chemistry of metal complexes with nitrogen oxide (NO) ligands, especially those of iron porphyrin derivatives and nitric oxide. This is the result of the important roles the ligands play in biological systems which include, among others, neurotransmission, vascular dilation, cytotoxicity, and activation of biochemical processes.[1] Recently a NO-bound ferric hemoprotein was found in a blood-sucking insect that uses the protein to aid in its need to obtain a blood meal.[2] There is of course, a biological production enzyme, NO-synthase, based on a heme protein.[3] Indeed, the biological roles of NO are so extensive that they have been the subject of two recent volumes in the *Methods in Enzymology* series.[4] It is clear that understanding of the biological functions has been greatly aided by earlier studies of the interaction of nitric oxide with iron porphyrinates that are cited below.

The focus in the first surge of interest in nitric oxide complexes was in understanding the bonding between metal and the diatomic ligand NO. The unusual nature of the geometry of the M−N−O linkage, which was found to be sometimes linear and sometimes bent,[5] is one important feature of the bonding in these species. The controlling factor in the bonding geometry is the electronic configuration, which in terms of the suggested Enemark and Feltham notation[5] can be expressed as $\{MNO\}^n$ where n is the number of d electrons on the metal plus the unpaired electron from NO. For five- or six-coordinate nitrosylmetalloporphyrin derivatives, when $n \leq 6$, as in the manganese(II) derivatives $[Mn(TTP)(NO)]$[6,7] and $[Mn(TPP)(4\text{-}MePip)(NO)]$[8] and the iron(III) derivatives $[Fe(OEP)(NO)]^+$ and $[Fe(TPP)(H_2O)(NO)]^+$,[9] the M−N−O linkage is linear. In these porphyrin derivatives, the five-coordinate derivatives have a high affinity for a sixth axial ligand. For cases where $n = 8$, as in five-coordinate $[Co(TPP)(NO)]$,[10] the Co−N−O linkage is strongly bent. Furthermore, there is little or no affinity for another axial ligand and only five-coordinate species are known.

[†] University of Notre Dame.

[‡] Present address: Faculté des Sciences de Monastir, 5000 Monastir, Tunisia.

[§] Emory University.

[⊗] Abstract published in *Advance ACS Abstracts*, June 15, 1997.

(1) Snyder, S. H. *Science* **1992**, *257*, 494. Butler, A. R.; Williams, D. L. H. *Chem. Soc. Rev.* **1993**, 233. Yu, A. E.; Hu, S.; Spiro, T. G.; Burstyn, J. N. *J. Am. Chem. Soc.* **1994**, *116*, 4117. Ignarro, L. J. *Circ. Res.* **1989**, *65*, 1. Moncada, S.; Palmer, R. M. J.; Higgs, E. A. *Pharmacol. Rev.* **1991**, *43*, 109.

(2) Ribeiro, J. M. C.; Hazzard, J. M. H.; Nussenzveig, R.; Champagne, D.; Walker, F. A. *Science* **1993**, 539−541.

(3) Richards, M. K; Clague, M. J.; Marletta, M. A. *Biochemistry* **1996**, *35*, 7772 and references cited therein.

(4) *Nitric Oxide Parts A and B in Methods in Enzymology*; Packer, L., Ed.; Academic Press: San Diego, CA, 1996; Vols. 268 and 269.

(5) Enemark, J. H.; Feltham, R. D. *Coord. Chem. Rev.* **1974**, *13*, 339.

S0002-7863(96)03871-1 CCC: $14.00

The intermediate system, where $n = 7$, is exemplified by iron(II) derivatives. Five-coordinate [Fe(TPP)(NO)][11] and the six-coordinate derivatives [Fe(TPP)(1-MeIm)(NO)][12] and [Fe(TPP)(4-MePip)(NO)][13] (two crystalline forms) have intermediate values for the Fe−N−O angle. In these derivatives, it is clear that the coordinated nitric oxide ligand exerts a strong trans effect; the Fe−N bond distances trans to NO are ≥0.20 Å longer than normal. Moreover, there are large variations in the trans Fe−N distance as seen in the two forms of [Fe(TPP)(4-MePip)(NO)],[13] where these distances are 2.328(10) and 2.463(7) Å.

The M−N(NO) bond distances in the porphyrin derivatives are all quite short and vary in the order Mn(II) ≃ Fe(III) < Fe(II) < Co(II). These distances, along with the observation that all of the above complexes are low-spin species, are manifestations of the strong M → NO π-bonding. The π-accepting NO ligand forms either one π-bond (in the bent systems) or two π-bonds (in the linear systems). The nitrite complexes of iron(II)[14] and iron(III)[15−17] porphyrins are also found to have electronic structures that are only consistent with the N-bound nitrite ligands acting as strong π-accepting ligands. The five-coordinate iron(II) complex $[Fe(TpivPP)(NO_2)]^{-}$[14] is especially noteworthy. This complex has a quite short Fe−$N(NO_2)$ bond and an unusually large quadrupole splitting; both result from the extremely strong M → $N(NO_2)$ π-bonding which leads to strong differentiation between the two d_π orbitals of the iron(II) porphyrin.

To further explore these issues of bonding and electronic structure, we have prepared and characterized new (porphinato)iron(II) complexes that have nitric oxide and nitrite as the trans axial ligands. The syntheses of these {FeNO}^{7} complexes begins with iron(II) nitrite derivatives, and to avoid possible problems with reactions of coordinated nitrite seen in iron(III) systems,[18] picket fence porphyrin was used as the porphyrin ligand. The complexes have been characterized by a combination of spectroscopic methods and by X-ray diffraction studies. Two different crystalline forms of [K(222)][Fe(TpivPP)(NO_2)(NO)] have been prepared; the two structural forms further demonstrate the importance of relative axial ligand orientation effects in defining electronic structure in iron porphyrins.

Experimental Section

General Information. All manipulations were carried out under argon using a double-manifold vacuum line, Schlenkware, and cannula techniques. Chlorobenzene was purified by washing with sulfuric acid and then distilled over P_2O_5. Pentane was distilled over CaH_2. Toluene, benzene, and hexanes were distilled over sodium benzophenone. KNO_2 was recrystallized twice from distilled water, dried overnight at 75 °C, and stored under argon. Kryptofix-222 (Aldrich) was recrystallized from benzene and stored under argon in the dark. NO gas was purified by passing it through a KOH column or through 4A molecular sieves immersed in a dry ice/ethanol slush bath to remove higher oxides of nitrogen.[19] The free base, *meso*-α,α,α,α-(*o*-pivalamidophenyl)porphyrin (H_2TpivPP) and the corresponding iron(III) chloro and triflate derivatives were synthesized by literature methods.[20,21]

UV−vis spectra were recorded on a Perkin-Elmer Lambda 6 spectrometer and IR spectra on a Perkin-Elmer model 883 as KBr pellets and Nujol mulls. EPR spectra were obtained at 77 K on a Varian E-12 spectrometer operating at X-band. Both the strong- and weak-field Mössbauer spectrometers were operated in a constant acceleration mode with a transmission arrangement and have been described elsewhere.[22] Zero velocity of the Mössbauer spectra are referred to the centroid of the room temperature spectrum of a metallic iron foil. Samples of $[Fe(TpivPP)(NO_2)(NO)]^{-}$ for Mössbauer spectroscopy were prepared by immobilization of the crystalline material (crystals not ground) in paraffin wax (m.p. 78° C) in the dry box.

Preparation of [K(222)][Fe(TpivPP)(NO_2)(NO)]. [Fe(TpivPP)$(SO_3CF_3)(H_2O)$] (100 mg, 0.08 mmol) and about 1 mL of zinc amalgam were stirred for 1 h under argon in 10 mL of C_6H_5Cl. This deep red solution ([Fe^{II}(TpivPP)]) was then filtered into a second solution that was made by stirring (overnight) 300 mg of Kryptofix-222 (0.8 mmol) and 207 mg of KNO_2 (2.4 mmol) in 10 mL of C_6H_5Cl. A stream of NO gas was passed (for about 15 min) through this red-yellow solution of the pentacoordinate iron(II) species $[Fe(TpivPP)(NO_2)]^{-}$.[14]

The color changes to light red as a result of forming the hexacoordinate product $[Fe(TpivPP)(NO_2)(NO)]^{-}$. Single crystals of this complex were prepared by slow diffusion of dry pentane into the chlorobenzene solution. A mass of single crystals of the desired complex and excess KNO_2 and Kryptofix-222 resulted. Crystals for X-ray analysis were selected from the mass under the microscope. Mössbauer samples were prepared by collecting the mass on a fritted-glass filter, washing with pentane, and then washing with a small quantity of degassed H_2O, leaving bulk crystalline material. Alternatively, the mass was washed directly in the reaction vessel and wash solvents were removed by cannula filtration. To our knowledge, each bulk sample was homogenous in iron(II) product. However, two different crystalline species, each with the same ligand set, were obtained. The initial crystalline form was obtained several times over the course of several months, followed approximately 1 year later by the production of a second crystalline form. This second crystalline form has then been exclusively obtained in all subsequent experiments. UV−vis in C_6H_5Cl λ_{max} (log ϵ) 544 (4.01), 426 (4.96). EPR (frozen chlorobenzene solution): $g_x \approx 2.1$, $g_y \approx 2.07$, and $g_z = 2.01$. IR (KBr) (form 1): ν (NO) 1616 (m) cm^{-1}; ν (NO_2^-) 1380 (w) cm^{-1}, 1310 (m) cm^{-1}. IR (Nujol) (form 2): ν (NO) 1668 (s) cm^{-1}; ν (NO_2^-) 1346 (m) cm^{-1}, 1305 (m) cm^{-1}.

X-ray Diffraction Studies of $[Fe(TpivPP)(NO_2)(NO)]^{-}$.[23] Both crystalline forms of this complex have been used in X-ray diffraction studies. A summary of crystal data, intensity collection data, and least-squares refinement parameters of these new hexacoordinate iron(II) porphyrin species are given in Tables 1 and S1 (Supporting Information).

Investigations on the first crystalline form were carried out at 124 K using graphite-monochromated Mo Kα radiation on an Enraf-Nonius CAD4 diffractometer. Data were processed with the Blessing suite[24]

(6) Abbreviations: Porph, a generalized porphyrin dianion; TpivPP, the dianion of *meso*-α,α,α,α-tetrakis(*o*-pivalamidophenyl)porphyrin; TPP, dianion of *meso*-tetraphenylporphyrin; T *p*-OCH_3PP, dianion of *meso*-tetrakis(*p*-methoxyphenyl)porphyrin; TTP, the dianion of *meso*-tetratolylporphyrin; OEP, the dianion of octaethylporphyrin; TMP, the dianion of *meso*-tetramesitylporphyrin; OBTPP, dianion of octabromotetraphenylporphyrin; TDCPP, dianion of *meso*-tetrakis(2,6-dichlorophenyl)porphyrin; Kryptofix-222 or 222, 4,7,13,16,21,24-hexaoxa-1,10-diazabicyclo[8.8.8]hexacosane; 4-MePip, 4-methylpiperidine; Py, pyridine; HIm, imidazole; PMS, pentamethylene sulfide; 1-MeIm, 1-methylimidazole; EPR, electron paramagnetic resonance; N_p, porphyrinato nitrogen.

(7) Scheidt, W. R.; Hatano, K.; Rupprecht, G. A.; Piciulo, P. L. *Inorg. Chem.* **1979**, *18*, 292.
(8) Piciulo, P. L.; Rupprecht, G.; Scheidt, W. R. *J. Am. Chem. Soc.* **1974**, *96*, 5293.
(9) Scheidt, W. R.; Lee, Y. J.; Hatano, K. *J. Am. Chem. Soc.* **1984**, *106*, 3191.
(10) Scheidt, W. R.; Hoard, J. L. *J. Am. Chem. Soc.* **1973**, *95*, 8281.
(11) Scheidt, W. R.; Frisse, M. E. *J. Am. Chem. Soc.* **1975**, *97*, 17.
(12) Piciulo, P. L.; Scheidt, W. R. *J. Am. Chem. Soc.* **1976**, *98*, 1913.
(13) Scheidt, W. R.; Brinegar, A. C.; Ferro, E. B.; Kirner, J. F. *J. Am. Chem. Soc.* **1977**, *99*, 7315.
(14) Nasri, H.; Wang, Y.; Huynh, B. H.; Scheidt, W. R. *J. Am. Chem. Soc.* **1991**, *113*, 717.
(15) Nasri, H.; Goodwin, J. A.; Scheidt, W. R. *Inorg. Chem.* **1990**, *29*, 185.
(16) Nasri, H.; Wang, Y.; Huynh, B. H.; Walker, F. A.; Scheidt, W. R. *Inorg. Chem.* **1991**, *30*, 1483.
(17) Nasri, H.; Haller, K. J.; Wang, Y.; Huynh, B. H.; Scheidt, W. R. *Inorg. Chem.* **1992**, *31*, 3459.
(18) Finnegan, M. G.; Lappin, A. G.; Scheidt, W. R. *Inorg. Chem.* **1990**, *29*, 181.
(19) Dodd, R. E.; Robinson, P. L. *Experimental Inorganic Chemistry*; Elsevier: New York, 1957; pp 233−234.
(20) Collman, J. P.; Gagne, R. R.; Halbert, T. R.; Lang, G; Robinson, W. T. *J. Am. Chem. Soc.* **1975**, *97*, 1427.
(21) Gismelseed, A.; Bominaar, E. L.; Bill, E.; Trautwein, A. X.; Nasri, H.; Doppelt, P.; Mandon, D; Fischer, J.; Weiss, R. *Inorg. Chem.* **1992**, *31*, 1845.
(22) Kretchmar, S. A.; Teixeira, M.; Huynh, B. H.; Raymond, K. N. *Biol. Met.* **1988**, *1*, 26.

Table 1. Crystallographic Details

	form 1	form 2
formula	$[K(O_6N_2C_{18}H_{36})][Fe(O_4N_8C_{64}H_{64})(NO)(NO_2)]\cdot(C_5H_{12})_{0.36}\cdot(C_6H_5Cl)_{0.64}$	$[K(O_6N_2C_{18}H_{36})][Fe(O_4N_8C_{64}H_{64})(NO)(NO_2)]\cdot(C_5H_5Cl)_{0.5}\cdot(H_2O)_{0.5}$
FW	1654.7	1622.0
a, Å	33.34(3)	13.070(12)
b, Å	18.80(5)	21.502(19)
c, Å	27.10(4)	31.848(29)
β, deg	95.30(9)	98.21(5)
V, Å^3	16916(56)	8858(25)
Z	8	4
space group	$P2_1/c$	$P2_1/n$
D_c, g/cm^3	1.301	1.22
F(000)	7024	3436
μ, mm^{-1}	0.317	0.308
crystal dimens, mm	0.80 × 0.30 × 0.23	0.59 × 0.43 × 0.39
diffractometer	CAD4	FAST
λ, Å	0.71073	0.71073
T, K	124	127
total data colld	27181	
no. of unique data	26673 ($R_{int} = 0.0386$)	26458 ($R_{int} = 0.029$)
no. of unique obsd data [$I > 2\sigma(I)$]	18562	9398
final *R* indices [$I > 2\sigma(I)$]	$R_1 = 0.0947$; $wR_2{}^a = 0.1904$	$R_1 = 0.094$; $wR_2{}^b = 0.107$
final *R* indices (for all data)	$R_1 = 0.1498$; $wR_2{}^a = 0.3179$	

[a] Based on F^2. [b] Based on *F*.

of data reduction programs. Very narrow diffraction profiles were used to avoid reflection overlap. The structure was solved in the monoclinic space group $P2_1/c$ with the program MULTAN. There are two $[Fe(TpivPP)(NO_2)(NO)]^-$ anions and two potassium Kryptofix-222 counterions in the asymmetric unit of structure. The final structural refinement was made with F^2 data with the program SHELXL-93,[25] in which all data collected were used, including reflections with negative intensities. One porphyrin, one cryptand, and one chlorobenzene molecule are completely ordered. There is disorder in the axial ligands of the second porphyrin molecule. The oxygen atom of the nitrosyl ligand is disordered on two positions with refined occupancies of 0.77(4) and 0.23(4). The NO_2 group displays linkage isomerism as it is coordinated through an oxygen atom (60%) or a nitrogen atom (40%). The coordinated atom (O, N) occupies the same site in both cases, and the scattering factor of nitrogen was used for this fully occupied atom. A *tert*-butyl group of a picket occupies two alternate positions with converged occupancies of 0.66(2) and 0.34(2). One strand of the second cryptand molecule is disordered on two positions with refined occupancy coefficients converged to 0.727(10) and 0.273(10). A pentane and chlorobenzene molecule alternately occupy the same site. The occupancy of the pentane molecule converged to 0.728(7). The chlorobenzene molecule was refined as a rigid body with an occupancy of 0.272(7) at convergence. All non-hydrogen atoms were refined anisotropically except the minor component of the disordered *tert*-butyl group, the minor component as well as several atoms of the major component of the disordered cryptand strand, and the partially occupied chlorobenzene molecule. All hydrogen atoms were idealized with the standard SHELXL-93 idealization methods. At convergence, $R_1 = 0.095$ and $wR_2 = 0.190$.[26] A final difference Fourier map was judged to be significantly free of features with the largest positive peak having a height of 0.90 e/Å^3. Complete listings of atomic coordinates, thermal parameters, and final hydrogen atom coordinates are given in the Supporting Information (Tables S2, S3, and S4).

A second form was subsequently obtained with the same crystallization methods (and the same experimenter). A dark purple crystal of this form with dimensions 0.39 × 0.43 × 0.59 mm was mounted on the end of a glass fiber. All measurements were performed with graphite-monochromated Mo Kα radiation ($\bar{\lambda} = 0.710\ 73$ Å) on an Enraf-Nonius FAST area detector diffractometer at 127 K. Our detailed methods and procedures for small molecule X-ray data collection with the FAST system have been described.[27] Data were corrected for Lorentz and polarization factors but not for absorption. A total of 26 458 observed reflections ($F_o \geq 2.0\sigma(F_o)$) were measured and averaged to 9398 unique reflections.

The structure of this crystalline form was solved in the centrosymmetric space group $P2_1/n$ with the direct methods program MULTAN. The E-map and subsequent difference Fourier syntheses led to the location of all heavy atoms. A chlorobenzene and a water solvent molecule were found; the two molecules share the same region of the unit cell and must be alternately populated (occupancies were fixed at 0.5 for both molecules). Thus the complete formula for the structure is $[K(222)][Fe(TpivPP)(NO_2)(NO)]\cdot{}^1/_2C_6H_5Cl\cdot{}^1/_2H_2O$. A minor disorder was found for the nitro and nitrosyl axial ligands. The occupancies of the second positions of the two oxygen atoms of the nitro group and the oxygen atom of the nitrosyl were fixed at 0.1. The orientation of each minor moiety is approximately orthogonal to its corresponding major one. After full-matrix least-squares refinement was carried to convergence, a difference Fourier suggested possible locations for most hydrogen atoms of the Kryptofix-222 and the porphyrin. Hydrogen atoms were included in subsequent cycles of the least-squares refinement as fixed, idealized contributions (C−H = 0.95 Å, N−H = 0.90 Å, $B(H) = B(C,N) \times 1.3$). Final cycles of full-matrix least-squares refinement used anisotropic temperature factors for all heavy atoms except (i) the oxygen atoms of the second positions of the nitro and nitrosyl groups: O(5b), O(6b), and O(7b), and (ii) C(63),

(23) Programs used in this study include (a) MADNES routines for FAST data collection (J. W. Pflugrath, Cold Spring Harbor, and A. Messerschmidt, Max-Plank-Institute für Biochemie, Martinsried, unpublished) and data reduction the program ABSURD (I. Tickle, Birbeck College, and P. Evans, MRC, unpublished), (b) direct method program MULTAN (Main, P.; Hull, S. E.; Lessinger, L.; Germain, G.; Declerq, J. P.; Woolfson, M. M. MULTAN, a system of computer programs for the automatic solution of the crystal structures from X-ray diffraction data. Universities of York, U.K., and Louvain, Belgium), (c) Zalkin's FORDAP for difference Fourier syntheses, (d) local modified least-square refinement (Lapp, R. L.; Jacobson, R. A. ALLS, a generalized crystallographic least-squares program. National Technical Information Services IS-4708 UC-4, Springfield, VA), (e) Busing and Levy's ORFFE and ORFLS and Johnson's ORTEP2 and ORTEP3, (f) atomic form factors from: Cromer, D. T.; Mann, J. B. *Acta Crystallogr., Sect. A* **1968**, *24*, 321, real and imaginary corrections for anomalous dispersion in the form factor of iron and the potassium and the chlorine atoms from Cromer, D. T.; Liberman, D. J. *J. Chem. Phys.* **1970**, *53*, 1891, and scattering factors for hydrogen from Stewart, R. F.; Davidson, E. R.; Simpson, W. T. *J. Chem. Phys.* **1959**, *42*, 3175.

(24) Blessing, R. H. *Crystallogr. Rev.* **1987**, *1*, 3.

(25) Sheldrick, G. M. *J. Appl. Crystallogr.* Manuscript in preparation.

(26) $R_1 = \sum||F_o| - |F_c||/|F_o|$ and $wR_2 = \{\sum[w(F_o{}^2 - F_c{}^2)^2]/\sum[wF_o{}^4]\}^{1/2}$ (for refinement with F^2 data). The conventional *R* factor R_1 is based on *F*, with *F* set to zero for negative F^2. The criterion of $F^2 > 2\sigma(F^2)$ was used only for calculating R_1. *R* factors based on F^2 (wR_2) are statistically about twice as large as those based on *F*, and *R* factors based on ALL data will be even larger. $wR_2 = [\sum w(|F_o| - |F_c|)^2/\sum w(F_o)^2]^{1/2}$ (for refinement with data on *F*).

(27) Scheidt, W. R.; Turowska-Tyrk, I. *Inorg. Chem.* **1994**, *33*, 1314.

(28) Mu, X. H.; Kadish, K. M. *Inorg. Chem.* **1988**, *27*, 4720.

(29) Nasri, H.; Scheidt, W. R. Manuscript in preparation.

Table 2. Electronic Spectral Data for Selected Iron(II) and Iron(III) Tetraarylporphyrins[a]

complex	λ_{max} (nm) Soret region (log ε)	α, β region (log ε)					ref
			A. Five-Coordinate Iron(II)				
[Fe(TPP)(NO)][b]	406 (4.97)	475 (sh)		538 (4.00)		604 (3.45)	11
[Fe(TpivPP)(NO)][c]	407 (5.15)	477 (sh) (4.35)		539 (4.12)		607 (3.62)	17
[Fe(TMP)(NO)][d]	408 (4.96)	477 (sh)		539 (3.04)		611 (3.84)	28
$[Fe(TpivPP)(NO_2)]^-$ [c]	444 (5.12)	433 (sh) (4.94)		543 (sh) (3.89)	567 (4.02)	608 (3.59)	14
			B. Six-Coordinate Iron(II)				
$[Fe(TpivPP)(NO_2)(NO)]^-$ [c]	410 (sh) (4.91)	426 (4.96)	478 (sh) (4.14)	544 (4.01)			this work
$[Fe(TpivPP)(NO_2)(Py)]^-$ [c]	413 (sh) (4.83)	430 (5.23)		533 (4.21)	560 (sh) (3.66)	653 (2.83)	29
$[Fe(TpivPP)(NO_2)(PMS)]^-$ [c]	418 (sh) (4.88)	432 (5.07)		537 (4.18)	558 (sh) (3.81)	653 (3.12)	29
[Fe(TPP)(NO)(1-MeIm)][b]		415 (5.26)	460 (4.26)	545 (3.99)	580 (sh) (3.78)	643 (3.05)	12
			C. Five-, Six-Coordinate Iron(III)				
$[Fe(TpivPP)(NO_2)_2]^-$ [c]	364 (sh)	426 (5.11)	464 (sh)	553 (4.15)			15
$[Fe(TpivPP)(NO_2)(Py)]$[c]		422 (5.26)	459 (sh)	550 (4.11)			16
$[Fe(TPP)(NO)]^+$ [d,e]	379 (sh)	411 (4.85)		546 (4.01)		680 (sh)	28
$[Fe(TPP)(NO_2)(NO)]$[b]		433 (5.34)	510 (sh) (3.70)	545 (4.20)	577 (sh) (3.70)		36a
$[Fe(T\ p\text{-}OCH_3PP)(NO_2)(NO)]$[c]		437		549	586		*f*
$[Fe(TpivPP)(NO_2)(NO)]$[c]		432		542	581		*g*

[a] All spectra were taken at 25 °C. [b] Chloroform solution. [c] Chlorobenzene solution. [d] Dichloromethane solution. [e] Thin-layer spectroelectrochemical oxidation of the corresponding Fe(II) species. [f] Ellison, unpublished. [g] Nasri, unpublished.

C(64), and C(68) of the chlorobenzene solvent. At convergence, $R_1 = 0.094$ and $wR_2 = 0.107$ and the final data/variable ratio was 8.8.[26] A final difference Fourier map was judged to be significantly free of features with the largest positive peak having a height of 0.89 e/Å^3. Final atomic coordinates, anisotropic and isotropic thermal parameters for all heavy atoms, and fixed hydrogen atom coordinates are available in the Supporting Information (Tables S5, S6, and S7).

Results and Discussion

The synthesis of the novel complex anion $[Fe(TpivPP)(NO_2)(NO)]^-$ with two (trans) axial nitrogen oxide ligands is straightforward but requires substantial experimental care owing to the oxygen sensitivity of the product and intermediates in solution. The preparative reaction makes use of five-coordinate [K(222)][Fe(TpivPP)(NO$_2$)],[14] prepared in situ by reaction of [Fe^{II}(TpivPP)] with an excess of Kryptofix-222-solubilized KNO_2, followed by reaction with gaseous NO. The complex has been characterized by IR, UV−vis, EPR, and Mössbauer spectroscopy as well as by single-crystal structure determinations. The product, $[Fe(TpivPP)(NO_2)(NO)]^-$, appears quite stable once it has been isolated (as single crystals) although crystals of $[K(222)][Fe(TpivPP)(NO_2)(NO)]\cdot{}^1/_2C_6H_5Cl\cdot{}^1/_2H_2O$ do seem to effloresce solvent but *not* NO on long standing (>3 mo). Grinding the crystalline product, however, does appear to cause a loss of NO. In solution, in the presence of excess nitrite ion, the complex appears to be easily oxidized to initially yield the bis(nitro)iron(III) complex $[Fe(TpivPP)(NO_2)_2]^-$. The instability of solutions of the nitrite−iron(III) porphyrin system has been previously noted,[18] and it is to be expected that other products will also ensue. In the absence of oxygen, the $[Fe(TpivPP)(NO_2)(NO)]^-$ anion is a stable species that persists in solution as a six-coordinate complex. As shown in Table 2 and Figure 1, the spectral properties of this six-coordinate, mixed-ligand complex are distinctively different from all other known iron(II) or -(III) tetraarylporphyrinate derivatives containing nitrite or nitrosyl ligands. It can be seen from the data in Table 2 that a Soret band near 430 nm is characteristic of six-coordinate species containing a good π-accepting ligand. The UV−vis spectral data thus show that it is highly unlikely that either of the axial ligands of $[Fe(TpivPP)(NO_2)(NO)]^-$ dissociates in chlorobenzene solution. The strong similarities of the solid-state and frozen solution EPR spectra are also highly suggestive concerning this point.

Two crystalline forms of $[Fe(TpivPP)(NO_2)(NO)]^-$ have been obtained and studied by X-ray diffraction. The two crystalline forms differ in the relative orientation of axial ligands and solvent content; the effect of ligand orientation appears to have significant effects on the electronic structure. As further detailed below, solid-state Mössbauer spectra of the two crystalline forms clearly show that the two are different not only at the single-crystal level but at the level of the bulk samples. Crystals of form 1 contain two independent complex anions in the asymmetric unit of structure. Their structures are illustrated in Figures 2 (anion 1) and 3 (anion 2). The ORTEP diagram shown for anion 2 also displays the disorder that results from the linkage isomerism of binding the nitrite anion. The common labeling scheme used for the two anions is given in Figure 4, which is an alternate view of anion 1. The structure of the complex anion found in crystal form 2 is given in Figure 5. The ligands to iron are the four porphinato nitrogen atoms, the nitrogen atom of nitric oxide, and a donor atom from nitrite ion. In two complex anions, the nitrite ion donor atom is solely nitrogen, while in the third case, the axial NO_2^- ligand exhibits disorder with the donor atom being either a nitrogen or an oxygen atom. In this complex, there is also a correlated disorder in the *tert*-butyl group of one of the pickets. It is seen that the nitrite anion is in the ligand binding pocket of picket fence porphyrin in all three complex anions.

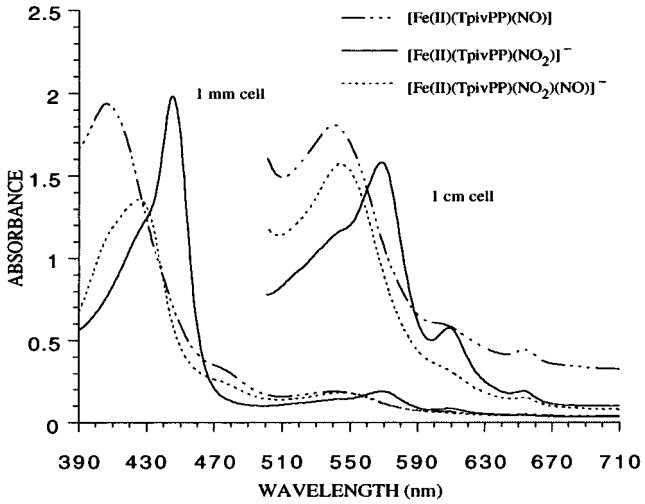

Figure 1. UV−vis spectra of $[Fe(TpivPP)(NO_2)(NO)]^-$, $[Fe(TpivPP)(NO_2)]^-$, and [Fe(TpivPP)(NO)] (chlorobenzene solution, approximately equivalent concentrations).

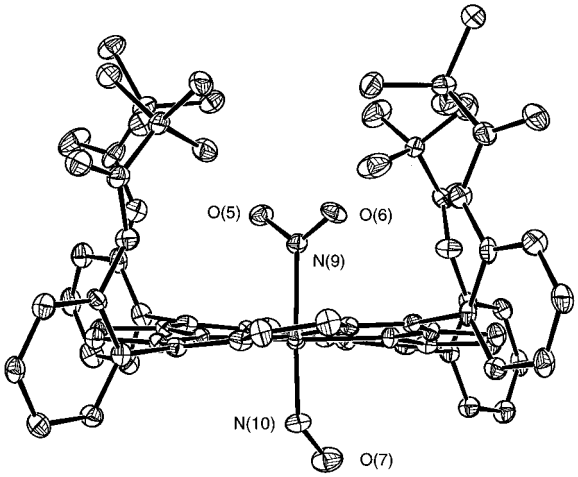

Figure 2. ORTEP diagram illustrating the structure of the $[Fe(TpivPP)(NO_2)(NO)]^-$ anion (30% probability ellipsoids, form 1, anion 1). The two ordered axial ligands have been labeled. The angle between the NO_2 and the Fe−N−O planes is 85.4°.

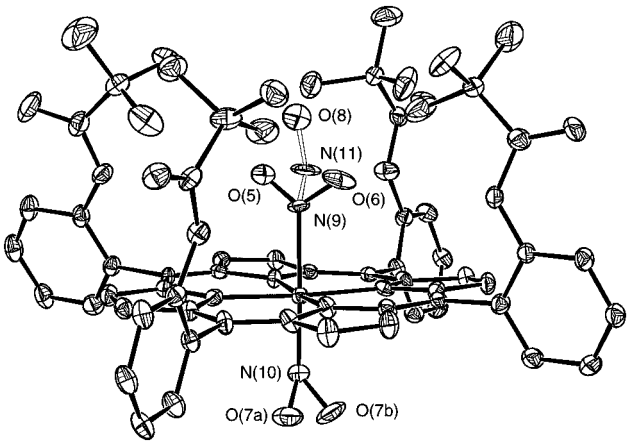

Figure 3. ORTEP diagram illustrating the structure of the $[Fe(TpivPP)(NO_2)(NO)]^-$ anion (30% probability ellipsoids, form 1, anion 2). The disorder in the two axial ligands is shown.

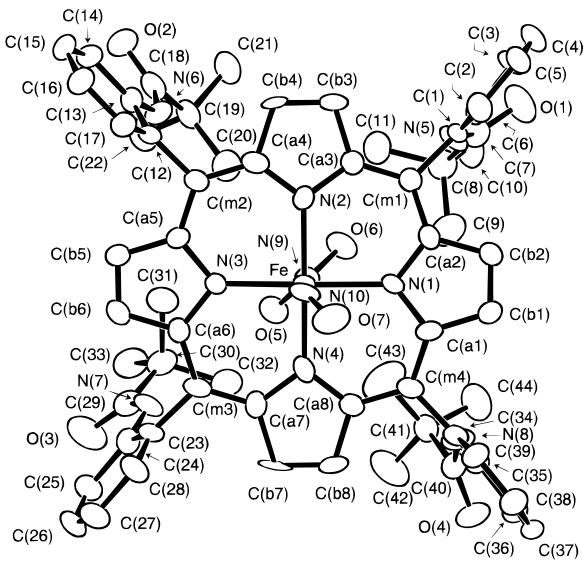

Figure 4. ORTEP diagram illustrating the labeling scheme used for the $[Fe(TpivPP)(NO_2)(NO)]^-$ anions in form 1. Anion 1 (50% probability ellipsoids) is depicted; identical labels are used in both anions.

Complete listings of bond distances and bond angles in the complex anions, cations, and solvent molecules are given in the Supporting Information. Table 3 summarizes bond distances, angles, and the FeNO−NO_2 dihedral angle in the coordination group of the three independent complex anions. Differences in bond distances between the three anions in $[Fe(TpivPP)(NO_2)(NO)]^-$ are small, and only those of the Fe−N(NO) distances are possibly significant. In all three complex anions, the nitric oxide bonds in a bent fashion; the Fe−N−O angles are all near 137°. Figure 6 gives formal diagrams for the three porphinato cores in the two crystalline forms. The diagrams display the displacement of each atom (in units of 0.01 Å) in the core from the mean plane of the 24-atom core. The porphinato ring in all anions shows S_4 ruffling. In all three complex anions, the iron atom is slightly displaced (0.08−0.10 Å) out of the plane toward the nitric oxide ligand. The diagrams also display averaged[30] values of each chemically distinct bond distance and angle type in the core. Finally, Figure 6 gives the orientation of the NO_2^- and FeNO planes with respect to the porphinato core. The projection of the NO_2^- plane onto the porphinato core is seen to lead to near bisecting of an N_p−Fe−N_p angle in both crystalline forms. However, in each of the form 1 complexes, the angle between the NO_2^- and FeNO planes is seen to be near 90°, while in form 2 the analogous angle is 21°.

Metal complexes with nitrogen oxide ligands that have nitrogen atoms in two different oxidation states are relatively rare, and only a few have been structurally characterized. All such complexes have nitrosyl/nitrite ligand mixtures.[31−37] Although $[Fe(TpivPP)(NO_2)(NO)]^-$ should thus be described as an unusual species, it should be noted that the analogous iron(III) species $[Fe(TPP)(NO_2)(NO)]$ has been known for some time,[36] although it has not been structurally characterized. All of the $[Fe(TpivPP)(NO_2)(NO)]^-$ complex anions are found to have a coordinated bent nitrosyl; two are found to have trans N-bound nitrite exclusively, while the third has an unusual linkage isomerism disorder with both O- and N-bound nitrite. All of the previously structurally characterized mixed ligand species have N-bound nitrosyl ligands; however, many have an O-bound (nitrito) rather than an N-bound (nitro) NO_2^- ligand. The metal−nitrosyl (M−N−O) angle is generally close to linear. The majority of the known mixed complexes would be considered low-valent species. A major point of interest in such mixed species is their potential in metal nitrosyl oxidations of organic substrates.[38] Interestingly, many, but not all, of the mixed ligand species can be prepared by oxygen atom transfer reactions of coordinated nitrite and nitric oxide.[31,32] The only iron complex[32] is an iron(III) complex with cis nitrosyl and

(30) The numbers in parentheses following each averaged value is the estimated standard deviation calculated on the assumption that all averaged values are drawn from the same population.

(31) Kriege-Simondsen, J.; Elbaze, G.; Dartiguenave, M.; Feltham, R. D.; Dartiguenave, Y. *Inorg. Chem.* **1982**, *21*, 230. Kriege-Simondsen, J.; Feltham, R. D. *Inorg. Chim. Acta* **1983**, *71*, 185.

(32) Ileperuma, O. A.; Feltham, R. D. *Inorg. Chem.* **1977**, *16*, 1876.

(33) Wester, D.; Edwards, R. C.; Busch, D. *Inorg. Chem.* **1977**, *16*, 1055.

(34) (a) Abraham, F.; Nowogrocki, G.; Sueur, S.; Bremard, C. *Acta Crystallogr., Sect. C* **1983**, *C39*, 838. (b) Carrondo, T.; Rudolph, P. R.; Skapski, A. C.; Thornback, J. R.; Wilkinson, G. *Inorg. Chim. Acta* **1977**, *24*, L95.

(35) Lukehart, C. M.; Troup, J. M. *Inorg. Chim. Acta* **1977**, *22*, 81. Wilson, R. D.; Bau, R. *J. Organomet. Chem.* **1980**, *191*, 123. Calderon, J. L.; Cotton, F. A.; DeBoer, B. G.; Maretinez, N. *J. Chem. Soc., Chem. Commun.* **1971**, 1476. Bell, L. K.: Mason, J.; Mingos, D. M. P.; Tew, D. G. *Inorg. Chem.* **1983**, *22*, 3497.

(36) (a) Yoshimura, T. *Inorg. Chim. Acta* **1984**, *83*, 17. (b) Settin, M. F.; Fanning, J. C. *Inorg. Chem.* **1988**, *27*, 1431.

(37) (a) Fajer, J. Personal communication. (b) Kadish, K. M.; Adamian, V. A.; Caemelbecke, E. V.; Tan, Z.; Tagliatesta, P.; Bianco, P.; Boshi, T.; Yi, G.-B.; Khan, M.; Richter-Addo; G. B. *Inorg. Chem.* **1996**, *35*, 1343−1348. (c) Ford, P. C.; Miranda, K.; Lee, B.; Bourasssa, J.; Kudo, S. *Abstracts of Papers*, 211th National Meeting of the American Chemical Society, New Orleans, LA; American Chemical Society: Washington, DC, 1996; Abstract INOR 626. (d) Bohle, D. S.; Gopodson, P. A.; Smith, B. D. *Polyhedron* **1996**, *15*, 3147.

(38) Richter-Addo, G. B.; Legzdins, P. *Metal Nitrosyls*; Oxford University Press: New York, 1992.

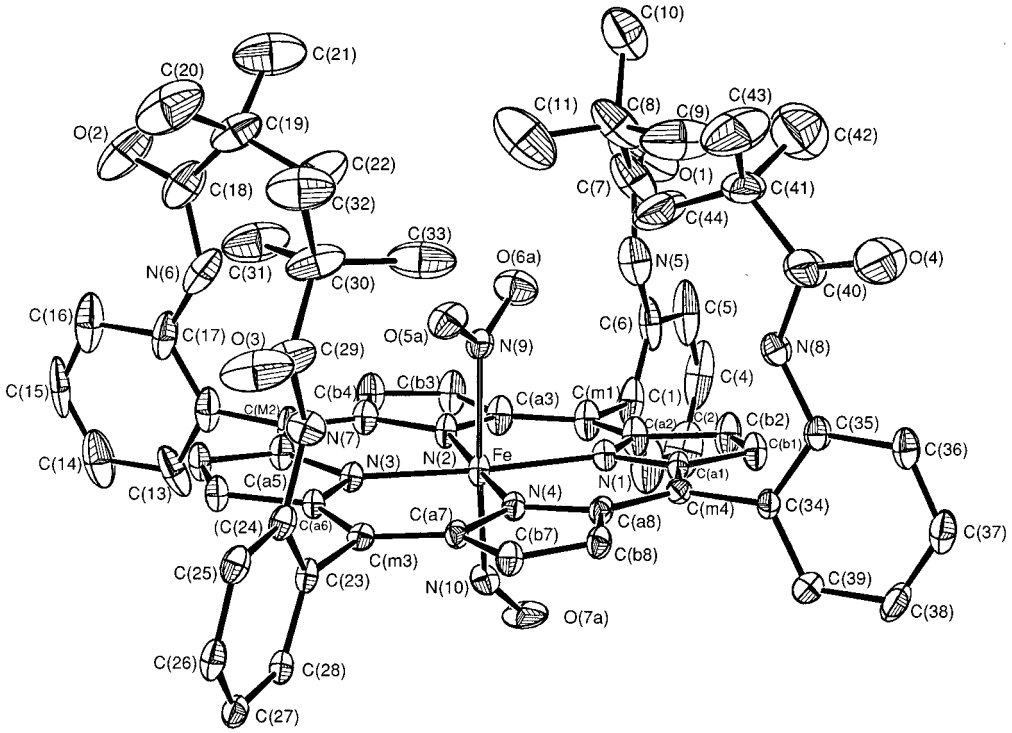

Figure 5. ORTEP diagram illustrating the molecular structure of $[Fe(TpivPP)(NO_2)(NO)]^-$ (30% probability ellipsoids, form 2). The labels of the crystallographically unique atoms are shown along with the values of the bond distances in the coordination group. The near parallel orientation of the nitrite ion plane and the iron−nitrosyl plane is evident (the dihedral angle is 20.9°).

Table 3. Selected Bond Distances (Å) and Angles (deg) for $[Fe(TpivPP)(NO_2)(NO)]^-$ [a,b]

	form 1, anion 1	form 1, anion 2	form 2
	Lengths[c]		
Fe−N(1)	2.003(6)	1.992(6)	1.984(6)
Fe−N(2)	1.993(6)	1.991(6)	1.983(6)
Fe−N(3)	1.996(6)	2.008(6)	1.982(6)
Fe−N(4)	1.962(6)	1.994(6)	1.996(6)
Fe−N(9)	2.086(8)	2.080(8)	2.060(7)
Fe−N(10)	1.792(8)	1.774(8)	1.840(6)
N(9)−O(5)	1.246(7)	1.17(2)	1.202(8)
N(9)−O(6)	1.245(8)	1.21(2)	1.259(9)
N(10)−O(7)	1.176(8)	1.156(10)	1.134(8)
	Angles[d]		
Fe−N(9)−O(5)	120.3(5)	122.9(11)	122.0(6)
Fe−N(9)−O(6)	121.8(5)	123.6(9)	120.7(5)
Fe−N(10)−O(7)	137.4(6)	139.4(7)	137.4(6)
O(5)−N(9)−O(6)	117.8(6)	113.0(13)	117.2(7)
	Dihedral Angles[d]		
$FeNO-NO_2$	85.4	76.2	20.9
$N_pFeN-NO_2$	44.1	41.4	44.0
$N_pFeN-FeNO$	41.3	35.2	25.2

[a] Estimated standard deviations of least significant digits are given in parentheses. [b] In cases where disorder is present, bond lengths and angles presented represent the major nitro component. [c] Value in angstroms. [d] Value in degrees.

nitrite ligands and two dithiocarbamate ligands. The complexes closest in structure to the present case are an octahedral Cr(I) macrocyclic complex and a ruthenium(III) porphyrin. The Cr(I) complex has a linear nitrosyl and a trans nitro ligand; the two axial Cr−N distances are quite different with Cr−N(NO) = 1.679(5) Å and $Cr-N(NO_2)$ = 2.204(5) Å.[33] The ruthenium system, which has been independently synthesized by at least four different groups, has a linear nitrosyl and a trans O-bound NO_2^-.[37]

Prior investigations of nitrite-complexed iron porphyrinates[14−17,29] have made clear that the nitrite ion plays a dominant role in the bonding. In all of these derivatives the nitrite ion has nearly the same absolute orientation: the projection of the nitrite ion plane onto the porphinato core effectively bisects a porphyrin N_p-Fe-N_p bond angle. Analysis of Mössbauer spectra of these nitrite complexes, obtained in an applied magnetic field, requires an unusual rotation of the $\tilde{g}$ and $\tilde{A}$ tensor axes in order to fit the spectra. This strongly suggests that the two d_π orbitals are perpendicular to the heme plane and between the $Fe-N_p$ directions.[16,17,39] In other words, the planes of the two d_π orbitals do not correspond to the directions taken from the heme geometry. However, this rather unusual orientation is exactly that required for iron π-donation to nitrite. Moreover, in five-coordinate [K(222)][Fe(TpivPP)(NO_2)], the single axial nitrite ligand provides a sufficient axial ligand field to yield a low-spin iron(II) complex, consistent with a strong π-acid ligand.

Although the evidence is perhaps not as direct, M → L π-bonding is also significant for the nitrosyl ligand. Furthermore, in the six-coordinate iron(II) systems, the nitrosyl ligand has a strong trans effect. Thus, while it is certainly to be expected that the present nitronitrosyl complexes will be low spin, it is not clear which of the axial ligands, nitric oxide or nitrite (or both), will predominate in defining the axial ligand bonding. Two limiting possibilities, consistent with the synthetic chemistry, can be enumerated. If NO dominates the axial π-bonding to the near exclusion of nitrite, it would be expected that the trans $Fe-N(NO_2)$ distance would be quite long as the NO ligand in this iron(II) derivative showed its usual structural trans effect. If both axial ligands were to exhibit strong π-accepting behavior, it is to be expected that two axial ligands should be found in planes orthogonal to each other, so as to maximize the M → L π-bonding.

In the actual case, the structures in the two crystalline forms of $[Fe(TpivPP)(NO_2)(NO)]^-$ show different bonding geometries from the limiting possibilities given above. The geometries appear to reflect differences in bonding of the axial ligands; furthermore, the differences appear to be manifested in physical

(39) We assume that the *z* direction is the heme normal. This assumption has been confirmed by single-crystal EPR measurements (S. Lloyd, Emory University, unpublished observations).

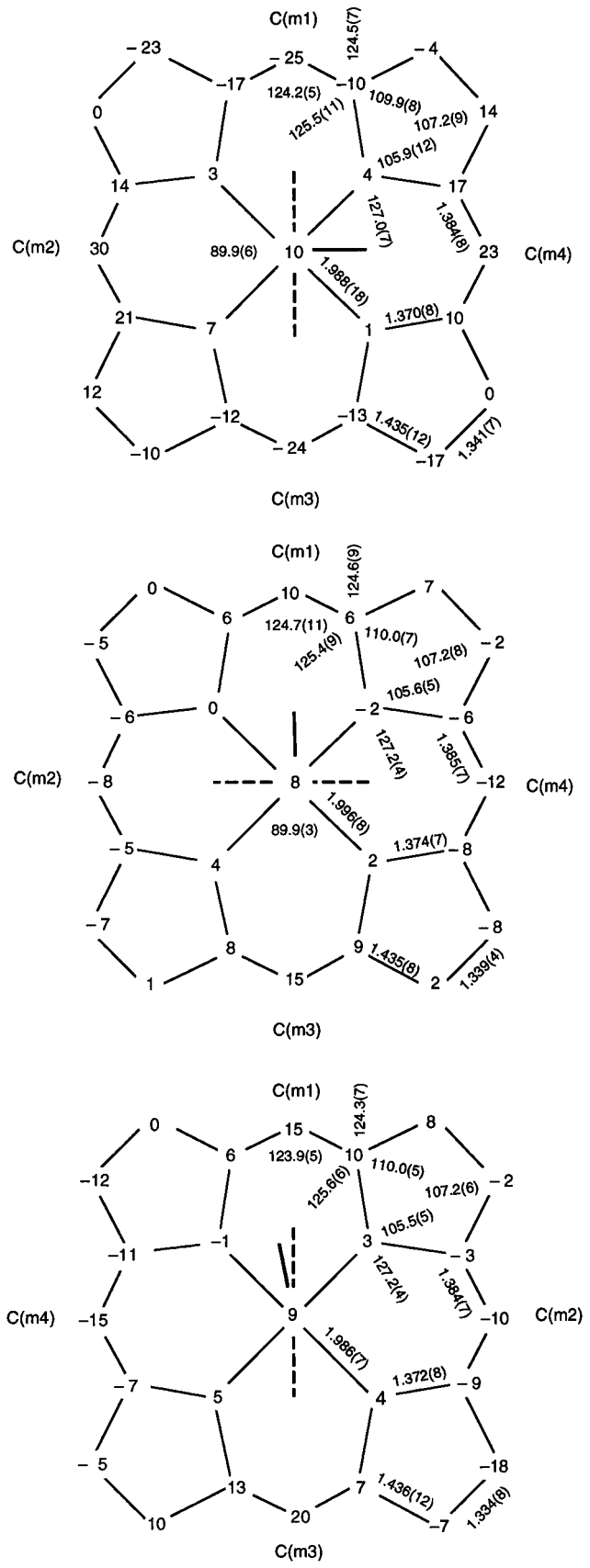

Figure 6. Formal diagram of the porphinato core of the $[Fe(TpivPP)(NO_2)(NO)]^-$ illustrating the displacement of each unique atom from the mean plane of the 24-atom porphinato core in units of 0.01 Å. Negative values of displacement are toward the nitro ligand. Also displayed on the diagram are the averaged values of each type of bond distance and angle in the porphinato core. The relative orientation of the two axial ligands with respect to the porphyrin core (and to each other) are also schematically displayed. Top: form 1, anion 1. Middle: form 1, anion 2. Bottom: form 2.

properties and in the electronic structure at iron. The NO group geometries are well determined in both crystalline forms, although two of the nitrosyl ligand descriptions are marred by minor crystallographic disorder. The observed Fe−N−O angles are similar and bent (137°) as expected for these iron(II) {FeNO}^{7} species. The two form 1 anions have the two axial ligands in near orthogonal planes with both ligand planes close to bisecting an N_p−Fe−N_p angle. The two axial ligands in crystals of form 2 are close to being in the same plane, but again, the two ligand planes nearly bisect an N_p−Fe−N_p angle; these dihedral angles are summarized in Table 3. The absolute orientations observed for the axial ligands suggest that they exert a prominent role in defining the orientation of the d_π orbitals as was previously noted for nitroiron(III) species.[16,17]

The distances and angles of Table 3 may be compared with the observed values for nitro- and nitrosylmetalloporphyrin derivatives given in Table 4. Several generalizations are apparent. The Fe−N_p bond distances are comparable to those of the other low-spin derivatives reported in Table 4. The observed Fe−N−O angles are smaller than those previously observed in the several iron(II) species. The data given in Table 4 suggest that Fe−N(NO) bond lengths might increase slightly upon change from five- to six-coordination, but those of the nitronitrosyl derivatives are clearly longer (by 0.08−0.12 Å) than those found in other nitrosyliron(II) derivatives. Comparison of the Fe−N(NO_2) distances in $[Fe(TpivPP)(NO_2)(NO)]^-$ with the values for the nitroiron(II) or -iron(III) derivatives presented in Table 4 shows that these distances are significantly longer (by ∼0.13 Å). Thus both types of axial distances are found to have similar, increased lengths compared to appropriate reference complexes. Nitric oxide appears to exert at most a modest trans effect in the nitronitrosyl complexes unlike the other six-coordinate nitrosyliron(II) complexes.

Thus, the structural data for the two forms of $[Fe(TpivPP)(NO_2)(NO)]^-$ are consistent with relatively strong NO bonding, though probably weaker than in the previously characterized nitrosyliron(II) derivatives. The axial nitrite ion bonding is also probably slightly weaker than in other studied nitrite complexes. It is reasonable to ascribe this decreased bonding to competition between the two strong axial π-accepting ligands. The most significant difference in the three species is that of the relative axial ligand orientations; bond distances are quite similar, suggesting that the various species have equivalent electronic structures. However, infrared and Mössbauer spectra provide evidence for real differences in electronic structure (and hence bonding) in the two crystalline forms. The differences in electronic structure, however, must be small in overall energy terms.

The solid-state IR spectrum of form 1 shows bands from the NO ligand (1616 cm^{-1}) and the nitrite ion (1380 and 1310 cm^{-1}). Form 2 also shows bands from the same moieties but at different frequencies: the band assigned to the NO ligand is at 1668 cm^{-1}, while the bands arising from the nitrite ion are at 1346 and 1305 cm^{-1}. NO stretching frequencies seen in nitrosyliron(II) porphyrin derivatives are a sensitive reporter of the bonding at iron. The NO stretching frequency found for five-coordinate $[Fe(TpivPP)(NO)]$[17] is 1665 cm^{-1}, and that for five-coordinate $[Fe(TPP)(NO)]$ is 1670 cm^{-1}.[11,41] Bohle and Hung[40] have reported that the stretching frequencies for a number of different five-coordinate nitrosyliron(II) derivatives range from 1675 to 1705 cm^{-1}. Differences appear to be qualitatively related to ease of oxidation of the metal. Most importantly, there is a significant effect on the NO stretching frequency of adding a trans sixth ligand. The addition of an

(40) Bohle, D. S.; Hung, C.-H. *J. Am. Chem. Soc.* **1995**, *117*, 9584.
(41) Wayland, B. B.; Olson. L. W. *J. Am. Chem. Soc.* **1974**, *96*, 6037.

Table 4. Summary of Coordination Group Geometry for Nitrosyl and Nitro Metalloporphyrin Derivatives

Metal Nitrosyl Derivatives

complex[a]	M−N_p	M−N_{NO}	∠MNO	M−L	ref
[Co^{II}(TPP)(NO)]	1.978(4)	1.833(53)	∼130		10
[Fe^{II}(TPP)(NO)]	2.001(3)	1.717(7)	149.2(6)		11
[Fe^{II}(TpivPP)(NO)]	1.981(26)	1.716(15)	143.8(17)		17
[Fe^{II}(OBTPP)(NO)]	1.986(23)	1.75(6)	146(2)		40
[Fe^{II}(TDCPP)(NO)]	2.004	1.703(8)	138.8(9)		40
[Fe^{II}(TPP)(NO)(1-MeIm)]	2.008(12)	1.743(4)	142.1(6)	2.180(4)	12
[Fe^{II}(TPP)(NO)(4-MePip)]	2.004(9)	1.721(10)	138.5(11)	2.328(10)	13
(second form)	1.998(10)	1.740(7)	143.7(6)	2.463(7)	13
[Mn^{II}(TTP)(NO)]	2.004(5)	1.641(2)	177.8(3)		7
[Mn^{II}(TPP)(NO)(4-MePip)]	2.027(3)	1.644(5)	176.2(5)	2.206(5)	7
[Fe^{III}(OEP)(NO)]$^+$	1.994(1)	1.644(3)	176.9(3)		9
[Fe^{III}(TPP)(NO)(H_2O)]$^+$	1.999(6)	1.652(5)	174.4(10)	2.001(5)	9
[Fe^{II}(TpivPP)(NO_2)(NO)]$^-$ (average of three values)	1.990(12)	1.802(34)	138.1(12)	2.075(5)	this work

Metal Nitro Derivatives

complex[a]	Fe−N_p	Fe−N_{NO_2}	M−L	ref
[Fe^{III}(TpivPP)(NO_2)$_2$]$^-$	1.992(1)	1.970(5)	2.001(6)	15
[Fe^{III}(TpivPP)(NO_2)(Py)]	1.985(3)	1.960(5)	2.093(5)	16
[Fe^{III}(TpivPP)(NO_2)(HIm)]	1.974(2)	1.949(10)	2.037(10)	16
[Fe^{III}(TpivPP)(NO_2)(SC_6HF_4)]$^-$	1.980(7)	1.990(7)	2.277(2)	17
[Fe^{II}(TpivPP)(NO_2)]$^-$	1.970(4)	1.849(6)		14
[Fe^{II}(TpivPP)(NO_2)(Py)]$^-$	1.990(15)	1.951(5)	2.032(5)	29
[Fe^{II}(TpivPP)(NO_2)(PMS)]$^-$	1.990(6)	1.937(3)	2.380(2)	29

[a] Formal oxidations states based on neutral NO.

imidazole ligand leads to a decrease in the NO stretch to 1625 cm^{-1}.[12,42] Moreover, the NO stretch appears to be quite sensitive to the Fe−L bonding trans to NO in [Fe(Porph)(NO)(L)]; an increased NO stretching frequency is seen as the trans interaction decreases. Scheidt and co-workers[13] found that two solid state forms of [Fe(TPP)(NO)(4-MePip)] had NO stretching frequencies of 1640 and 1653 cm^{-1}; these are correlated with the trans Fe−N(4-MePip) bond distances of 2.328(10) and 2.463(7) Å, respectively. Thus the fact that the two crystalline forms of [Fe(TpivPP)(NO_2)(NO)]$^-$ display differing NO stretching frequencies appears significant. The most straightforward, but perhaps not complete, interpretation of the solid-state IR differences is that the NO stretch variation reflects differences in the bonding to iron trans to NO. Thus the orthogonal orientation of the two ligand planes in the form 1 allows stronger π-bonding to both ligands than that in form 2 where the ligand planes are effectively parallel and nitric oxide bonding is more dominant.

Mössbauer spectra of a sample of form 2, recorded at temperatures ranging from 4.2 to 300 K in the absence or presence of a weak applied field (50 mT), show broad and featureless spectra, indicating that the electronic relaxation time of the complex is comparable to the Mössbauer sampling time (10^{-7} s). To obtain the characteristic hyperfine parameters, a spectrum was recorded at 4.2 K in the presence of a strong (8 T) magnetic field applied parallel to the γ-beam (Figure 7A). The strong field removes the degeneracy of the $S = {}^1/_2$ doublet such that the separation of the two energy levels is large in comparison to the sample temperature and the effects of electronic relaxation are minimized. The spectrum can then be analyzed by a spin Hamiltonian formalism commonly applied for the study of iron-containing proteins.[43] The solid line in Figure 7A is a theoretical simulation assuming fast electronic relaxation and using the following parameters: quadrupole splitting, $\Delta E_q = 1.2 \pm 0.2$ mm/s; isomer shift, $\delta = 0.35 \pm 0.05$ mm/s; asymmetry parameter, $\eta = 0.5 \pm 0.1$; magnetic hyperfine tensor, $A_{xx}/g_n\beta_n = -23$ T, $A_{yy}/g_n\beta_n = -(8.5 \pm 1.5)$ T, $A_{zz}/g_n\beta_n = +(14.5 \pm 0.5)$ T. The theoretical simulation was found to be insensitive to the parameter $A_{xx}/g_n\beta_n$ within the range −26 to −19 T. Except for the rhombicity detected in the *xy* plane, the hyperfine parameters determined for the [Fe(TpivPP)(NO_2)(NO)]$^-$ complex compare reasonably well in both signs and magnitudes with those observed for NO-bound heme proteins.[44−46] For example, the corresponding parameters

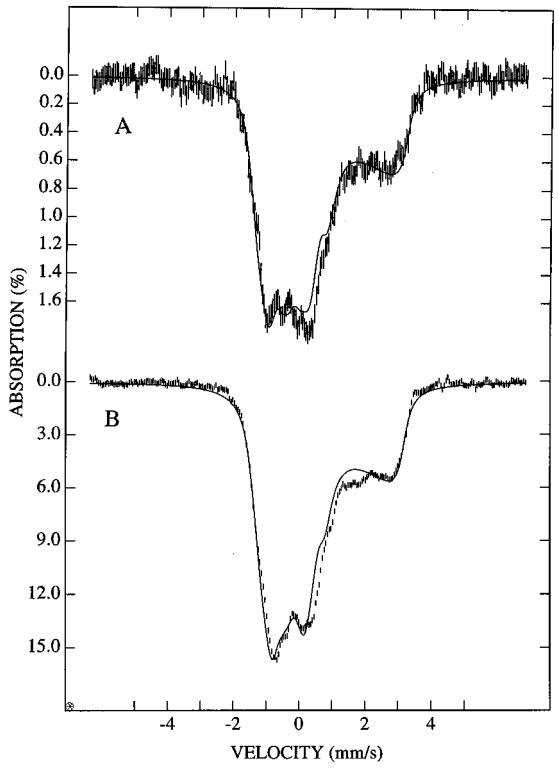

Figure 7. (A) Mössbauer spectrum of [K(222)][Fe(TpivPP)(NO_2)(NO)] (form 2) at 4.2 K in a parallel applied field of 8 T. The solid line shows the fit based on the parameters given in the text. (B) Mössbauer spectrum of [Fe(TPP)(NO)] at 4.2 K in a parallel applied field of 8 T. The solid line shows the fit based on the parameters given in the text.

(42) Maxwell, J. C.; Caughey, W. S. *Biochemistry* **1976**, *15*, 388.
(43) Huynh, B. H.; Kent, T. A. *Adv. Inorg. Biochem.* **1984**, *6*, 163.
(44) Liu, M.-C.; Huynh, B. H.; Payne, W. J.; Peck, H. D., Jr.; DerVartanian, D. V.; LeGall, J. *Eur. J. Biochem.* **1987**, *169*, 253.

observed for the NO-bound d_1 heme in the diheme cytochrome cd_1 nitrite reductase from *Thiobacillus denitrificans* are $\Delta E_q = 0.8$ mm/s, $\delta = 0.34$ mm/s, $A_{xx}/g_n\beta_n = A_{yy}/g_n\beta_n = -15$ T, and $A_{zz}/g_n\beta_n = +12$ T.[44] These values were suggested to indicate a substantial σ-electron donation from the NO ligand to the Fe d_{z^2} orbital and the π-electron back-donation from the Fe (d_{xy} and d_{xz}) to the NO. Most interestingly, a Mössbauer spectrum similar to that of the NO-bound d_1 heme is also observed for the NO-bound siroheme in the hemoprotein subunit of the *E. coli* sulfite reductase, where the siroheme is covalently linked to a [4Fe−4S] cluster.[45] These observations of similar Mössbauer spectra for NO-bound hemes of different macrocyclic structures suggest that the electronic structure of an NO-bound heme complex is predominantly determined by the Fe−NO moiety.

We have also studied the Mössbauer spectrum of a crystalline sample of the related five-coordinate nitrosyl complex [Fe(TPP)(NO)],[11,41] for which the electron relaxation was found to be relatively fast at 4.2 K. In the absence of an applied field, a broad quadrupole doublet is detected (Figure 8A). A least-squares fit of the data yields parameters ($\Delta E_q = 1.24 \pm 0.03$ mm/s and $\delta = 0.35 \pm 0.02$ mm/s) that are indistinguishable to those obtained from form 2 crystals of the nitronitrosyl complex, suggesting similar electronic structure for the two compounds. This similarity in electronic structure is further corroborated by the Mössbauer spectra recorded in strong applied fields. A spectrum of [Fe(TPP)(NO)] recorded at 4.2 K in an 8 T magnetic field applied parallel to the γ-beam is shown in Figure 7B for comparison with the spectrum of the six-coordinate nitronitrosyl complex recorded under the same conditions (Figure 7A). The spectra are almost identical showing only subtle differences. Analysis of the spectrum shown in Figure 7B yielded magnetic hyperfine parameters that are very similar to those of the six-coordinate complex. The solid line in Figure 7B is a theoretical simulation using the following parameters: $\Delta E_q = 1.24$ mm/s, $\delta = 0.35$ mm/s, $\eta = 0.32 \pm 0.05$, $A_{xx}/g_n\beta_n = -(25 \pm 4)$ T, $A_{yy}/g_n\beta_n = -(10 \pm 2)$ T, and $A_{zz}/g_n\beta_n = 13.2 \pm 0.5$ T. This strong resemblance in electronic structures observed for five-coordinate [Fe(TPP)(NO)] and six-coordinate [Fe(TpivPP)(NO_2)(NO)]$^-$ (form 2) complexes strongly suggests that nitric oxide is the predominant axial ligand in bonding in form 2.

In a sample of form 1, the electronic relaxation in the Mössbauer was found to be fast at high temperatures. Figure 8B shows the Mössbauer spectrum recorded for a bulk sample at 200 K. One major and one minor quadrupole doublet are observed, suggesting multiple iron environments. The major species (~75%, shown as a solid line in Figure 8B) has a broad quadrupole doublet with apparent parameters $\Delta E_q = 1.78$ mm/s and $\delta = 0.22$ mm/s; the value of δ at 4.2 K (corrected for the second-order Doppler shift) is expected to increase to about 0.28 mm/s. The 75% abundance in the Mössbauer agrees well with the independent estimate of 70% for the nitro linkage isomer species, supporting the idea that the Mössbauer sample and the single-crystal specimen represent the same sample. The samples of forms 1 and 2 are seen to have similar isomer shifts but significantly different quadrupole splittings and support the idea that there are differences in the electronic structure of the two crystalline forms. Unfortunately, the limited amount of the form 1 species available, along with the difficulties engendered by the multiple iron environments, did not allow a complete study in applied magnetic field. However, the value of the quadrupole splitting in form 1 halfway between that of five-coordinate [Fe(TPP)(NO)] (1.24 mm/s) and five-coordinate [Fe(TpivPP)(NO_2)]$^-$ (2.28 mm/s)[14] is strongly suggestive of a nitrite ion effect on the symmetry of the charge distribution at iron in the form 1 species.

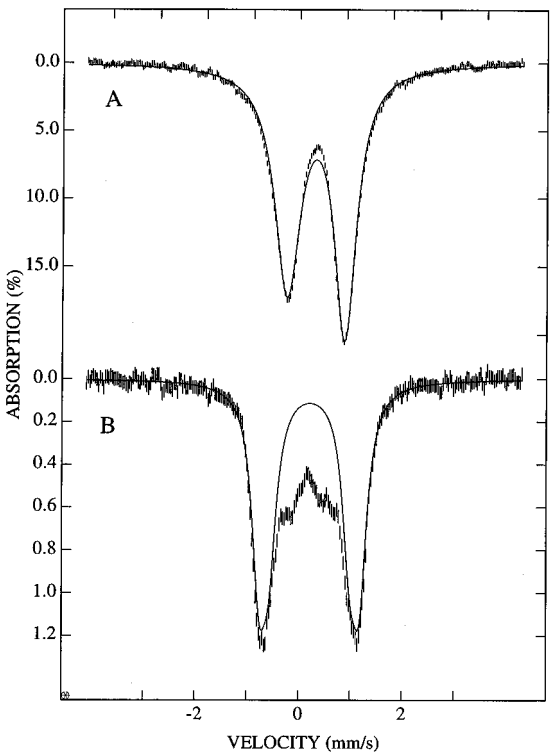

Figure 8. (A) Mössbauer spectrum of [Fe(TPP)(NO)] at 4.2 K in zero field. (B) Mössbauer spectrum of [K(222)][Fe(TpivPP)(NO_2)(NO)] (form 1) at 200 K in zero field.

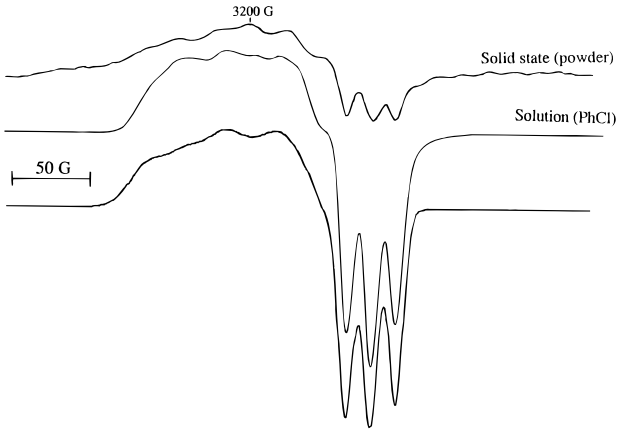

Figure 9. Solid-state and frozen chlorobenzene solution (77 K) EPR spectra of [K(222)][Fe(TpivPP)(NO_2)(NO)]. The simulated spectrum, using the parameters given in the text, is also displayed.

The low-spin iron(II) complex is paramagnetic owing to the unpaired electron derived from the NO ligand. The EPR spectrum of the complex (Figure 9) shows similar features in solution and in both solid state forms; in solution, hyperfine coupling from only one nitrogen atom (probably the nitrosyl nitrogen) is apparent. Figure 9 also shows a simulated spectrum. The following parameters were used in the spectral simulation: $g_x = 2.085$, $g_y = 2.032$, $g_z = 2.01$, a_x (^{14}N) = 24 G, $a_y = 16.5$ G, and $a_z = 16$ G. It is to be noted that the low-field portions of nitrosyliron porphyrin EPR spectra are particularly difficult to simulate due to possible interactions from porphinato nitrogen ligands.[47]

(45) Christner, J. A.; Münck, E.; Janick, P. A.; Siegel, L. M. *J. Biol. Chem.* **1983**, *258*, 11147.

(46) Costa, C.; Moura, J. J. G.; Moura, I.; Liu, M. Y.; Peck, H. D., Jr.; LeGall, J.; Wang, Y.; Huynh, B. H. *J. Biol. Chem.* **1990**, *265*, 14382.

(47) Henry, Y.; Ducrocq, C.; Drapier, J.-C.; Servent, D.; Pellat, C.; Guissani, A. *Eur. Biophys. J.* **1991**, *20*, 1.

The structures of the three complex cations, $[K(222)]^+$, are normal. Each potassium ion is coordinated by the usual six oxygen atoms and two nitrogen atoms of the cryptand ligand. One of the complex cations of form 1 has one disordered ethylene oxide chain, but the observed K−O and K−N distances are generally quite typical to that observed previously. The average value of the K−N distances is 3.01 Å, and the average K−O distance is 2.81 Å. (The range of K−O distances is 2.768(8)−2.860(8) Å.) ORTEP diagrams of the three cations are given in the Supporting Information.

Summary. The synthesis and characterization of two crystalline forms of the six-coordinate complex $[Fe(TpivPP)(NO_2)(NO)]^-$ are reported. Structurally, the two forms differ primarily in the relative orientation of the two axial ligands. In form 1, the two axial ligands are in perpendicular planes, which allows both ligands to more strongly bond to iron than in form 2. In this form, the two ligands are in essentially parallel planes and the nitric oxide ligand appears to be more dominant ligand to iron. These orientation differences are also manifested in differences in the Mössbauer and IR spectra.

Acknowledgment. We thank the National Institutes of Health for support of this research under Grant GM-38401 to W.R.S. and Grant GM-47295 to B.H.H. Funds for the purchase of the FAST area detector diffractometer were provided through NIH Grant RR-06709 to the University of Notre Dame.

Supporting Information Available: Tables S1−S11 giving complete crystallographic details, atomic coordinates, anisotropic temperature factors, fixed hydrogen atom positions, and complete listings of bond distances and angles for both crystallographic forms and Figures S1−S3 giving ORTEP diagrams of the K(222) cations (75 pages). See any current masthead page for ordering and Internet access instructions.

JA963871A